Electronic structures and magnetic properties of Zn- and Cd-doped AlN nanosheets: A first-principles study*

Rui-Lin Han(韩瑞林)[1,†], Shi-Min Jiang(姜世民)[1], and Yu Yan(闫羽)[2]

[1] College of Physics and Electronic Engineering, Shanxi University, Taiyuan 030006, China
[2] Key Laboratory of Physics and Technology for Advanced Batteries (Ministry of Education), Department of Physics, Jilin University, Changchun 130012, China

(Received 11 August 2016; revised manuscript received 17 October 2016; published online 20 December 2016)

In this paper, the magnetic properties, electronic structures and the stabilities of Zn/Cd incorporated two-dimensional AlN nanosheets are investigated by the first-principles method. Numerical results indicate that Zn and Cd substituting Al atom in AlN nanosheets introduce some holes into the 2p orbitals of the N atoms, and the holes mainly come from spin-down 2p orbitals of the N atoms. The magnetic moment of 1.0 μ_B is produced by Zn/Cd doping AlN nanosheets, and the main component of the magnetic moment of the system is contributed by the partially filled 2p states of the N atoms around the dopant. In particular, when Zn/Cd substituting Al atoms, the magnetic coupling is found to be ferromagnetic. We attribute the hole-mediated p–d interaction to the created ferromagnetic coupling. More importantly, the result of formation energy indicates that Al atom is more inclined to be replaced by Zn atom rather than Cd. This finding is beneficial to developing the spin electronic devices.

Keywords: AlN nanosheets, ferromagnetism, first-principles doping

PACS: 75.50.Gg, 75.50.Pp, 75.75.Lf **DOI:** 10.1088/1674-1056/26/2/027502

1. Introduction

With the successful isolation of graphene, other similar two-dimensional (2D) materials have aroused the wide interest of scientists due to their extraordinary structural, electronic properties as well as promising potential applications, such as BN,[1] GaX (X = S and Se),[2–5] MoS_2,[6,7] SnS_2,[8,9] TiS_3,[10,11] and AlN.[12,13] Among them, the AlN nanosheet has received considerable attention of researchers from the field of optics, electronics, photoelectronics and spintronics, for it enjoys the same honeycomb lattice structure as graphene and possesses outstanding properties.[14–25] In the field of spin electronics and magnetic devices, the AlN-based dilute magnetic semiconductor material is the most promising candidate. However, this pristine 2D material has no intrinsic magnetism as a semiconductor. Generally speaking, in order to obtain a set of integrated electric and magnetic spintronic devices, both spin and charge of electrons combined closely are needed to turn the semiconductor material into a magnetic material. For achieving its applications in spintronics, considerable efforts have been made to study the magnetic properties of these 2D materials in recent years. As is well known, the efficient and promising method of manipulating the magnetic properties of the nonmagnetic semiconducting material is substitutional doping. For example, it was reported that the substitution of Al with five transition metal (Cr, Mn, Fe, Co, and Ni) atoms can induce tunable magnetism in an AlN nanosheet.[18] However, the origin of the observed ferromagnetism remains controversial, since the doping TMs may form magnetic clusters or secondary phases.[26,27] Thus, the extrinsic origin cannot be excluded when magnetic transition metals are used as dopants, which is an obstacle to the practical applications of dilute magnetic semiconductors (DMSs). To avoid the extrinsic magnetism, much attention is being paid to exploring the effects of nonmagnetic element dopants. For instance, it was found that the substitution doping of B atom in the AlN (1120) film can induce magnetization and B dopants favor the surface layer.[19] Likewise, it was confirmed theoretically that a ferromagnetic property with Curie temperatures above room temperature is observed in Be-doped AlN monolayer.[20] More importantly, it was experimentally demonstrated that 1.2 at.%–7.9 at.% Mg-doped AlN films present ferromagnetic properties.[21] Correspondingly, it has been confirmed theoretically that Mg-doped AlN thin films can induce magnetism.[22] Meanwhile, some experimental and theoretical results have also been reported that the Cu-doped AlN films exhibit room-temperature ferromagnetism.[28–32] On the other hand, compared with conventional transition metal dopants, the nonmagnetic dopants have been a hot topic in recent years due to their high-temperature magnetism, which may be conducive to the mushroom growth of the spin electronics. To date, notwithstanding the magnetism in AlN nanosheets has been widely considered, a detailed understanding of the induced

*Project supported by the National Fundamental Fund of Personnel Training, China (Grant No. J1103210).
†Corresponding author. E-mail: hanruilin0116@sxu.edu.cn
© 2017 Chinese Physical Society and IOP Publishing Ltd

magnetism in Zn/Cd-doped AlN nanosheets has not been performed yet. What is more, previous studies have shown that Zn atom can be utilized as a p-type dopant in AlN.[33,34] In addition, Wu *et al.* experimental results also showed that Zn can be incorporated into AlN solid solution.[35] Consequently, it is very necessary to investigate the electronic structures and magnetic properties of substitutionally doped AlN nanosheets with Zn/Cd atom by first-principles studies.

2. Computational details

In this paper, the spin-polarized calculations are accomplished by means of the Vienna *ab initio* Simulation Package (VASP),[36,37] where the Perdew and Wang (PW91) formulation of the generalized gradient approximation (GGA) pseudopotential was used to depict the exchange and correlation interaction.[38] The electron–ion interactions were treated by the projector augmented wave potentials.[39] The kinetic energy cutoff of 400 eV was chosen for the plane-wave basis throughout the calculations. Moreover, the vacuum layer was set to be 15 Å for the 2D AlN nanosheets to eliminate the spurious interactions between the adjacent layers. The energy convergence threshold was set to be 10^{-4} eV, and both the cell and atomic relaxation were carried out until the force on each atom was less than 0.02 eV/Å. The valence electron configurations were Al ($3s^2 3p^1$), N ($2s^2 2p^3$), Zn ($3d^{10} 4p^2$), and Cd ($4d^{10} 5s^2$), respectively. In order to carry out a more accurate calculation of the doping system, we first considered the relaxed structural parameters of bulk AlN. The relaxed equilibrium lattice constants were $a = 3.126$ Å, $c = 5.017$ Å, consistent with experimental results and other theoretical values,[40–42] indicating the rationality of our computational methodologies. Correspondingly, in Figs. 1(a) and 1(b), the (4×4×1) and (6×6×1) supercells were constructed to delve the electronic structures and magnetic properties of one and two dopants (Zn/Cd) in AlN nanosheets, respectively. The 9×9×1 and 5×5×1 Monkhorst–Pack mesh were used to sample the Brillouin zone for the structural relaxations and physical properties, respectively.

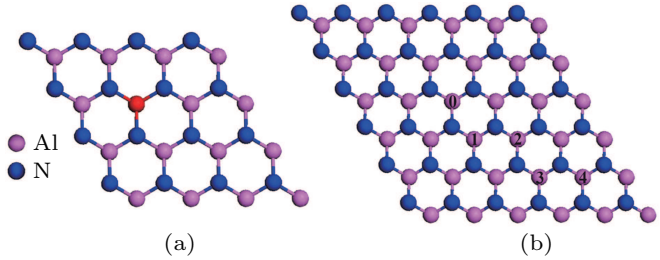


Fig. 1. (color online) Schematic views of structure for (a) 4×4×1 and (b) 6×6×1 AlN nanosheet supercells. Pink and dark blue spheres represent Al and N atoms, respectively. The substituted positions of *X* dopants are denoted by red in 4×4×1 nanosheet supercells and 0-4 in 6×6×1 nanosheet supercells, respectively.

3. Results and discussion

We first cut a 2D 4×4×1 unit cell directly into the (0001) plane of AlN optimized bulk wurtzite structure. After the total energy optimization, the relaxed Al-N bond length 1.785 Å in the case of the nanosheets is smaller than 1.898 Å of bulk structure, which accords well with previous theoretical results.[18,37] In addition, the AlN nanosheets are changed from the rippled surface to the planar graphene-like structure. These possible reasons are attributable to the lack of interlayer interaction in the nanosheets, where the bonding between Al and N atoms belongs to sp^2-hybridization and is stronger than the sp^3 bonding in bulk.

Then, figures 2(a) and 2(b) show the spin-polarized density of states (DOS) and band structure of pure AlN nanosheets. Figure 2(a) shows the main components of the valence band near the Fermi level by the 2p orbitals of N atoms; while the dominant components of the conduction bands come from Al-2s and N-2s state hybridization. It is worth noting that the state of spin-up and the state of spin-down are fully symmetric, which demonstrates that the pristine AlN nanosheets are nonmagnetic. From another point of view, as clearly seen in Fig. 2(b), the plotted band gap appearing between the top of the valence band and the bottom of the conduction band of the indirect band gap is 2.95 eV, located at the *G* point and *K* point, respectively, which is also consistent with previous calculations.[23,43,44] Thus, based on the above details of AlN nanosheets, the selected method is reliable for the following studies of Zn- and Cd-doped 2D AlN nanosheets.

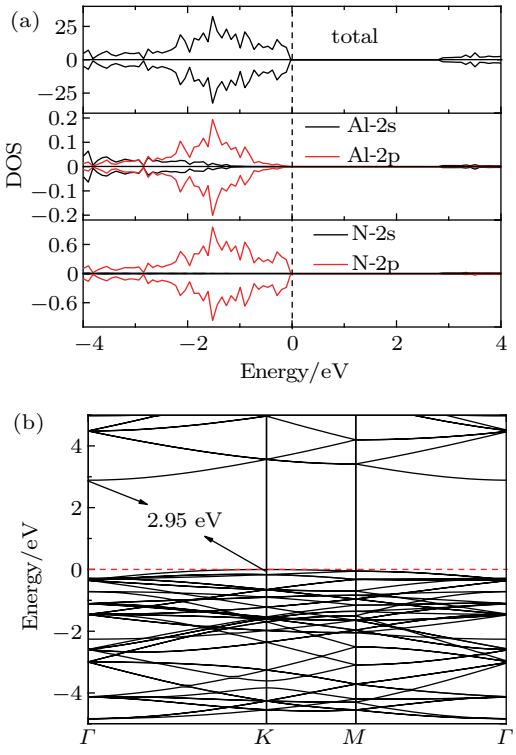


Fig. 2. (color online) (a) Total DOS and partial DOS of p and s states of the Al atoms and N atom, and (b) band structure for pure 2D AlN nanosheets. The Fermi energy is indicated by the dotted line.

Now, we begin to study X-doped AlN nanosheets (X = Zn and Cd) with 6.25% doping concentrations as shown in Fig. 1(a). Since the Zn and Cd atoms have similar radius to Al atoms, they are expected to occupy predominantly Al site in our calculation. The optimized structural and energy results and the magnetic moment distributions for Zn- and Cd-doped AlN nanosheets are given in Table 1. Our calculations show that the optimized bond lengths of Zn–N and Cd–N are found to be enlarged to 1.902 Å and 2.105 Å, respectively. This phenomenon can be explained to be due to the difference in radius between the doped atom and the substitution atom, in single X-doped AlN nanosheets, the atom radii of Zn (1.53) and Cd (1.71) are shorter than that of Al (1.82). For $Al_{15}ZnN_{16}$ and $Al_{15}CdN_{16}$ nanosheets, the calculations show that the total energy of spin polarization and spin unpolarization of the system are about 71.3 meV and 91.7 meV respectively, which fully proves that the state of spin polarization is a ground state. The local magnetic moments of each dopant, three N atoms of the closest to the dopant and other N atoms in $Al_{15}XN_{16}$ (X = Zn and Cd) nanosheets and the total magnetic moment of the system are also summarized in Table 1. The calculations demonstrate that the induced magnetic moment of Zn- or Cd-doped system is mostly offered from the closest N atoms around the dopant, and the magnetic moments of the other farther N atoms are one or two orders of magnitude smaller. It is worth noting that in spite of the smallness, the magnetic moments of the other N atoms can facilitate the magnetic coupling between the magnetic moments provided by the two dopants, which will be discussed below. Besides, the doped Zn or Cd atom also gives a small part for the moment. The residual magnetic moment is produced in the interstitial region around the doped atom and its nearest atoms. As a result, both Zn and Cd dopants produce a total magnetic moment of 1.00 μ_B in AlN nanosheets. Figures 3(a) and 3(b) show the distribution of magnetic moments, which accord well with the data given in Table 1. Analogous studies have been conducted in the past, such as Mg-, Be-, C-, and TM-doped AlN nanosheet,[18,20,22] Co-doped SnO_2 nanosheets,[45] and Cu-doped ZnO nanosheets.[46]

Table 1. Optimized X–N (X = Zn and Cd) bond lengths. The calculated values of total energy difference between spin-polarized (E_{spin}) and spin-unpolarized (E_{unspin}) states ($\Delta E = E_{spin} - E_{unspin}$). The values of magnetic moment of the doping atom (M_X), its nearest neighboring N atoms (M_{N1}) around the doping atom and other N atoms (M_{N2}), and the total magnetic moment of the nanosheets (M_{tot}).

System	X–N/Å	ΔE/meV	M_X/μ_B	M_{N1}/μ_B	M_{N2}/μ_B	M_{tot}/μ_B
$Al_{15}ZnN_{16}$	1.902	–71.3	0.025	0.430	0.160	1.000
$Al_{15}CdN_{16}$	2.105	–91.7	0.050	0.392	0.152	1.000

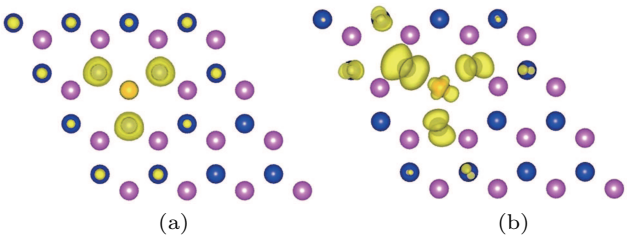


Fig. 3. (color online) Spin density distributions of the single X-doped AlN nanosheets in (a) $Al_{35}ZnN_{36}$ and (b) $Al_{35}CdN_{36}$. The yellow and green isosurfaces correspond to the majority- and minority-spin densities. Pink, dark blue and red balls represent Al, N, and doping atoms, respectively.

Figures 4(a) and 4(b) indicate that the total density of states of $Al_{15}ZnN_{16}$, a first neighboring N atom in the vicinity of Zn/Cd and corresponding the partial DOS of 3d and 4d states of Zn and Cd atom. It can be found from Fig. 4 that the low-valence state Zn/Cd substitution for Al atom gives rise to some holes in the 2p orbitals of the N atoms nearby dopant, causing the state of spin-up and the state of spin-down to be not symmetric, that is to say, the valence band has obvious spin splitting, resulting in a magnetic moment of 1.00 μ_B. The physical reasons for obtaining such a value of magnetic moment can be explained by analyzing the nature of Bader analysis. It notes that each N atom closest to Al atom has three valence electrons, and the N^{3-} anion has six p electrons without unpaired electrons, that is to say, the nearest neighboring three N atoms of the doped atom nominally carry 18 p-electrons in total. Since Zn atom has two electrons in its six p orbitals, the substitution of N atoms introduces one hole into Zn-doped AlN nanosheets. Similarly, Cd substitution of Al atom also induces one hole. Correspondingly, we find that Zn^{2+}/Cd^{2+} and the nearest neighboring three N atoms carry 17 p-electrons in total, resulting in a magnetic moment (1.00 μ_B) equal to that of unpaired electrons of 2p orbitals. What is more, the valence band is mainly composed of the 2p states of the N atoms, and a small part is provided by the d orbitals of the doped atom, which shows that the magnetic moment is mainly derived from partially occupied 2p states of the N atoms. Also from Fig. 4, we can find that the valence band has obvious spin splitting, leading to significant electronic properties of half-metallic state. This phenomenon is qualitatively consistent with the results of Mg-, Be-, C-, and TM-doped AlN nanosheets,[18,20,22] Co-doped SnO_2 nanosheets,[45] and Cu-doped ZnO nanosheets.[46]

In order to analyze the stabilities of Zn/Cd-doped AlN nanosheets, we calculate the formation energy, E_{form}. The for-

mation energy, $E_{\rm form}$, of an element X-doped system is acquired from the following formula: $E_{\rm form} = E(\rm Al_{15}XN_{16})$–$E(\rm Al_{16}N_{16}) + \mu_{Al} - \mu_X$,[47] where $E_{\rm AlN}(X)$ and $E_{\rm AlN}$ are the total energies of the AlN nanosheets containing a substitutional dopant X and the pristine AlN nanosheets in the same supercell; $\mu_{\rm Al}$ and μ_X are the total energies of metallic Al and X atoms, respectively. It should also be noted that the formation energies are determined as the Al-rich and N-rich conditions. Moreover, under the thermodynamic growth conditions, the upper and lower limits for the chemical potentials $\mu_{\rm N}$ and $\mu_{\rm Al}$ of N and Al are obtained from the equation $\mu_{\rm Al} + \mu_{\rm N} = \Delta H_{\rm f}$ (AlN), where $\Delta H_{\rm f}$ (AlN) is the formation enthaply of AlN nanosheets. Moreover, in the process of doping, in order to impede the second phases $\rm Zn_3N_2$ and $\rm Cd_3N_2$ between the dopant and host atoms from forming, the chemical potentials of Zn and Cd must be restricted by the inequalities $3\mu_{\rm Zn} + 2\mu_{\rm N} \leq \Delta H_{\rm f}$ [$\rm Zn_3N_2$] and $3\mu_{\rm Cd} + 2\mu_{\rm N} \leq \Delta H_{\rm f}$ [$\rm Cd_3N_2$]. The values of formation energy $E_{\rm f}$ of Zn- and Cd-doped AlN nanosheets in Al-rich and N-rich condition are summarized in Table 2. Following our calculations, it can be known that substitution for Al site becomes easy if the nanosheets are grown under N-rich conditions. Moreover, the Al atom is more inclined to be replaced by a Zn atom rather than Cd.

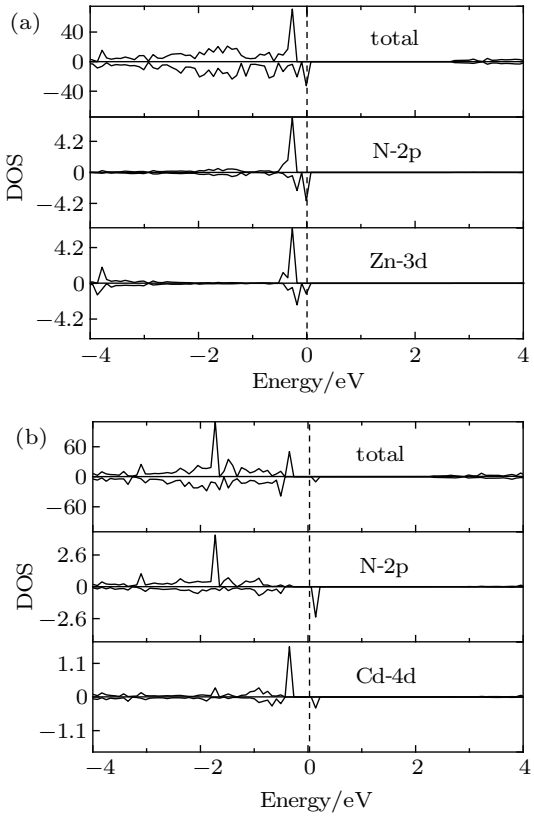


Fig. 4. DOSs of AlN nanosheets with single X substitution: (a) total DOS of $\rm Al_{15}ZnN_{16}$, partial DOS of 2p states of a first neighboring N atom around Zn atom and 3d states of a Zn atom, (b) total DOS of $\rm Al_{15}CdN_{16}$, partial DOS of 2p states of a first neighboring N atom around Cd atom and 4d states of a Cd atom, respectively. Fermi energy is indicated by the dashed vertical line.

Table 2. Values of formation energy $E_{\rm f}$ of Zn- and Cd-doped AlN nanosheets in Al-rich and N-rich condition.

X	$E_{\rm f}$ in Al-rich condition	$E_{\rm f}$ in N-rich condition
Zn	2.477	1.506
Cd	3.330	2.389

In order to discuss in depth the magnetic coupling between the moments induced by two doped Zn/Cd atoms, a larger $6\times6\times1$ supercell is set up. Four different configurations for doped system $\rm Al_{34}X_2N_{36}$ (X = Zn/Cd) are investigated, and the doping concentration is 5.6%. In the AlN nanosheets, one of the doped atoms is placed at site 0 position and another doped atom is placed at one of sites 1–4 as shown in Fig. 1(b). For simplicity, the four configurations are marked as (0,1), (0,2), (0,3), and (0,4). For the four configurations, the spin polarized calculations are implemented, and both ferromagnetic (FM) and antiferromagnetic (AFM) coupling between the moments produced by the two dopants are considered. The calculated optimized distance between two doped atoms, d_{X-X}, define the energy with respect to (0,2) configuration as the relative energy, $\Delta\varepsilon$, the magnetic moment, $M_{\rm tot}$, and the differences of the FM energy minus the AFM energy, i.e., $\Delta E_{\rm m} = E_{\rm FM} - E_{\rm AFM}$, for all the configurations of the doped system, are summarized in Table 3.

Table 3. Values of calculated distance (d_{X-X}) of two dopants, the relative energy $\Delta\varepsilon$ with respect to that of the (0,1) structure, the energy difference ($\Delta E_{\rm m}$) between FM and AFM states, $\Delta E_{\rm m} = E_{\rm FM} - E_{\rm AFM}$, and the total magnetic moment ($M_{\rm tot}$) in FM state for doped system $\rm Al_{34}X_2N_{36}$ (X = Zn and Cd).

System	Configurations $(0,i)$	d_{X-X}/Å	$\Delta\varepsilon$/meV	$\Delta E_{\rm m}$/meV	$M_{\rm tot}/\mu_{\rm B}$
$\rm Al_{34}Zn_2N_{36}$	(0,1)	3.126	88	–66	2.00
	(0,2)	5.414	0	–171.5	2.00
	(0,3)	8.271	82	–79.6	2.00
	(0,4)	10.828	108	–59.8	2.00
$\rm Al_{34}CdN_{36}$	(0,1)	3.126	118	–83.3	2.00
	(0,2)	5.414	0	–126.2	2.00
	(0,3)	8.271	220	–78.4	2.00
	(0,4)	10.828	200.1	–62	2.00

The results in Table 3 reveal that the energy of configuration (0,2) is lower than those of the other three configurations, which implies that the clustering effect is not apparent in Zn- and Cd-doped AlN nanosheets. Table 3 also shows that the $\Delta E_{\rm m}$ values of four configurations are negative, which implies that all ground states of $\rm Al_{34}X_2N_{36}$ (X = Zn/Cd) nanosheets, where the two dopants are located at the farthest possible distance in the nanosheets, are FM. What is more, the $\Delta E_{\rm m}$ values of the most stable configuration (0,2) for $\rm Al_{34}Zn_2N_{36}$ and $\rm Al_{34}Cd_2N_{36}$ are as large as -171.5 meV and -83.3 meV, respectively. This means that ferromagnetic state in Zn- and Cd-doped AlN nanosheets is likely to be achieved. The DOS of a

two-atom-doped system in FM state is similar to the DOS of single atom-doped AlN nanosheets, which shows that substitutional dopants at Al sites introduce holes into the spin-down 2p orbitals of the N atoms at the top of the valence band. In addition, it is the spin splitting of the valence band.

By combining the results obtained from DOS and spin density distribution, we can explain the ferromagnetic coupling between the magnetic moments introduced by the two doped atoms. From the DOSs in Figs. 4(a) and 4(b), the 2p orbitals of N atoms and the d orbitals of the dopant significantly overlap near the Fermi level, indicating there is a strong p–d hybridization interaction mechanism between them.[48] It can be revealed that the dopant and its nearest N atoms can couple with each other, causing the magnetic moments to be parallelly aligned by this strong interaction.[48,49] Indeed, as shown in Figs. 3(a) and 3(b), we find that the N atoms bonded to the dopant and the dopant are also spin polarized, meanwhile, the polarization direction is identical to that of the dopant. In other words, under the interaction of p–d hybridization, the spins of N atoms and the doped atom are parallel to each other. Moreover, the spatially extended p states of the N extend spin alignment to several neighboring N shells around the dopant. Consequently, the holes localized near the N atoms between two doped atoms in the nanosheets are polarized and have the same spin directions as shown in Figs. 5(a) and 5(b). These polarized holes can effectively regulate the long-range ferromagnetic coupling between the doped atoms.

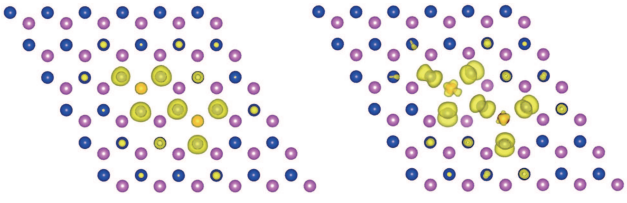


Fig. 5. (color online) Spin density distributions of double *X*-doped AlN nanosheets are shown in (a) $Al_{34}Zn_2N_{36}$ and (b) $Al_{34}Cd_2N_{36}$ FM state of configuration (0,2). The yellow and green isosurfaces correspond to the majority- and minority-spin densities. Pink, dark blue and red balls represent Al, N, and doping atoms, respectively.

4. Conclusions

In this work, through the theoretical calculations, the electronic structure and magnetic properties of a substitutional Zn/Cd dopant in 2D AlN nanosheet are systematically studied in detail. Our calculation results reveal that doped Zn/Cd in a 2D AlN nanosheet introduce some holes into 2p orbitals of the N atoms and the corresponding magnetic moments is 1.0 μ_B per supercell. The main component of the magnetic moment of the doped system is the 2p orbitals of the first neighboring N atoms in the vicinity of the dopant, with a small contribution from the Zn/Cd atom. Furthermore, the coupling effect between the magnetic moments due to the incorporation of Zn/Cd into the system is ferromagnetic coupling. According to the calculated DOS and spin density, we can conclude that the p–d interaction between the 2p states of the N atom and the d states of the dopant effectively tune the long-range FM coupling. Moreover, the formation energy calculations show that Al atom is more inclined to be replaced by Zn atom rather than Cd and could be realized under experimental conditions.

References

[1] Golberg D, Bando Y, Huang Y, Terao T, Mitome M, Tang C C and Zhi C Y 2010 *ACS Nano* **4** 2979
[2] Zhou Y B, Nie Y F, Liu Y J, Yan K, Hong J H, Jin C H, Zhou Y, Yin J B, Liu Z F and Peng H L 2014 *ACS Nano* **8** 1485
[3] Late D J, Liu B, Luo J, Matte H S S R, Rao C N R and Dravid V P 2012 *Adv. Funct. Mater.* **22** 1894
[4] Hu P A, Wen Z Z, Wang L F, Tan P H and Xiao K 2012 *ACS Nano* **6** 5988
[5] Hu P A, Wang L F, Yoon M, Zhang J, Feng W, Wang X N, Wen Z Z, Idrobo J C, Miyamoto Y, Geohegan D B and Xiao K 2013 *Nano Lett.* **13** 1649
[6] Lee Y H, Zhang X Q, Zhang W, Chang M T, Lin C T, Chang K D, Yu Y C, Wang J T, Chang C S, Li L J and Lin T W 2012 *Adv. Mater.* **24** 2320
[7] Tongay S, Zhou J, Ataca C, Lo K, Matthews T S, Li J, Grossman J C and Wu J 2012 *Nano Lett.* **12** 5576
[8] Wei R, Hu J, Zhou T, Zhou X, Liu J and Li J 2014 *Acta Mater.* **66** 163
[9] Chen P, Su Y, Liu H and Wang Y 2013 *ACS Appl. Mater. Interfaces* **5** 12073
[10] Dai J and Zeng X C 2015 *Angew. Chem. Int. Ed.* **54** 7572
[11] Iyikanat F, Sahin H, Senger R T and Peeters F M 2015 *J. Phys. Chem. C* **119** 10709
[12] Peng X Y and Ahuja R 2009 *Appl. Phys. Lett.* **94** 102504
[13] Tsipas P, Kassavetis S, Tsoutsou D, Xenogiannopoulou E, Golias E, Giamini S A, Grazianetti C, Chiappe D, Molle A, Fanciulli M and Dimoulas A 2013 *Appl. Phys. Lett.* **103** 251605
[14] Zhang X, Liu Z and Hark S 2007 *Solid State Commun.* **143** 317
[15] Liu P, Sarkar A D and Ahuja R 2014 *Comput. Mater. Sci.* **86** 206
[16] Valedbagi S, Fathalian A and Elahi S M 2013 *Opt. Commun.* **309** 153
[17] He H, Huang L, Xiao M, Fu Y, Shen X and Zeng J 2013 *J. Mater. Sci.: Mater. Electron.* **24** 4499
[18] Shi C M, Qin H W, Zhang Y J, Hu J F and Ju L 2014 *J. Appl. Phys.* **115** 053907
[19] Fan S W, Li W B, Huang X N, Li Z B and Pan L Q 2015 *Appl. Phys. Express* **8** 045802
[20] Bai Y J, Deng K M and Kan E J 2015 *RSC Adv.* **5** 18352
[21] Xiong J, Guo P, Guo F, Sun X and Gu H 2014 *Mater. Lett.* **117** 276
[22] Peng Y T, Xia C X, Zhang H, Wang T X, Wei S Y and Jia Y 2014 *J. Appl. Phys.* **116** 044306
[23] Zhang C W 2012 *J. Appl. Phys.* **111** 043702
[24] Zhang W X, Li T, Gong S B, He C and Duan L 2015 *Phys. Chem. Chem. Phys.* **17** 10919
[25] He H, Huang L, Xiao M, Fu Y, Shen X and Zeng J 2013 *J. Mater. Sci.: Mater. Electron.* **24** 4499
[26] Ney A, Ollefs K, Ye S, Kammermeier T, Ney V, Kaspar T C, Chambers S A, Wilhelm F and Rogalev A 2008 *Phys. Rev. Lett.* **100** 157201
[27] Kaspar T C, Droubay T, Heald S N, Nachimuthu P, Wang C M, Shutthanandan V, Johnson C A, Gamelin D R and Chambers S A 2008 *New J. Phys.* **10** 055010
[28] Luo J T, Li Y Z, Kang X Y, Zeng F, Pan F, Fan P, Jiang Z and Wang Y 2014 *J. Alloys Compd.* **586** 469
[29] Ran F Y, Subramanian M, Tanemura M, Hayashi Y and Hihara T 2009 *Appl. Phys. Lett.* **95** 112111
[30] Jiang L B, Liu Y, Zuo S B and Wang W J 2015 *Chin. Phys. B* **24** 027503
[31] Yan Z, Wu H L, Zheng R S and Xu B S 2015 *Materials Research Innovations* **19** 367

[32] Jia W, Han P D, Chi M, Dang S H and Xu B S 2007 *J. Appl. Phys.* **101** 113918

[33] Monemar M, Gislason H P and Lagerstedt O 1980 *J. Appl. Phys.* **51** 640

[34] Nepal N, Nakarmi M L, Jang H U, Lin J Y and Jiang H X 2006 *Appl. Phys. Lett.* **89** 192111

[35] Wu Z G, Zhang W B, Hu H R, Zuo S Y, Wang F Y, Yan P X, Wang J, Zhuo R F and Yan D 2014 *Mater. Lett.* **136** 95

[36] Kresse G and Hafner J 1993 *Phys. Rev. B* **47** 558

[37] Kresse G and Hafner J 1994 *Phys. Rev. B* **49** 14251

[38] Kresse G and Furthmuller J 1996 *Comput. Mater. Sci.* **6** 15

[39] Blöchl P E 1994 *Phys. Rev. B* **50** 17953

[40] Jonnard P, Capron N, Semond F, Massies J, Martinez-Guerrero E and Mariette H 2004 *Eur. Phys. J. B* **42** 351

[41] Wu Q Y, Huang Z G and Wu R 2007 *J Phys.: Condens. Matter* **19** 056209

[42] Valedbagi S, Fathalian A and Mohammad E S 2013 *Opt. Commun.* **309** 153

[43] Li S S, Zhang C W, Zhang R W, Li P, Li F, Yuan M, Ren M J, Ji W X and Wang P J 2014 *RSC Adv.* **4** 7500

[44] Zhang C W and Wang P J 2011 *Phys. Lett. A* **375** 3583

[45] Luan H X, Zhang C W, Li F, Li P, Ren M J, Yuan M, Ji W X and Wang P J 2014 *RSC Adv.* **4** 9602

[46] Li F, Zhang C W and Zhao M W 2013 *Physica E* **53** 101

[47] Guo H Y, Zhao Y, Lu N, Kan E J, Zeng X C, Wu X J and Yang J L 2012 *J. Phys. Chem. C* **116** 11336

[48] Shen L, Wu R Q, Pan H, Peng G W, Yang M, Sha Z D and Feng Y P 2008 *Phys. Rev. B* **78** 073306

[49] Long R and English N J 2009 *Phys. Rev. B* **80** 115212